Ultrafast Solvation Dynamics of Coumarin 153 in Imidazolium-Based Ionic Liquids

Lang, Bernhard Felix; Angulo, Gonzalo; Vauthey, Eric

Ultrafast Solvation Dynamics of Coumarin 153 in Imidazolium-Based Ionic Liquids

Bernhard Lang, Gonzalo Angulo,† and Eric Vauthey*

Department of Physical Chemistry, University of Geneva, CH-1211 Geneva 4, Switzerland

Received: December 23, 2005; In Final Form: March 30, 2006

The dynamic Stokes shift of coumarin 153 has been measured in two room-temperature ionic liquids, 1-(3-cyanopropyl)-3-methylimidazolium bis(trifluoromethylsulfonyl)imide and 1-propyl-3-methylimidazolium tetrafluoroborate, using the fluorescence up-conversion technique with a 230 fs instrumental response function. A component of about 10−15% of the total solvation shift is found to take place on an ultrafast time scale < 10 ps. The amplitude of this component is substantially less than assumed previously by other authors. The origin of the difference in findings could be partly due to chromophore-internal conformational changes on the ultrafast time scale, superimposed to solvation-relaxation, or due to conformational changes of the chromophore ground state in polar and apolar environments. First three-pulse photon-echo peak-shift experiments on indocyanine green in room-temperature ionic liquids and in ethanol indicate a difference in the inertial component of the early solvent relaxation of <100 fs.

1. Introduction

Over the past few years, room-temperature ionic liquids (RTIL) have attracted considerable attention as an alternative reaction medium for organic catalysis, for liquid−liquid extraction, and as ultralow volatility liquid matrixes.[1,2] Commonly, RTILs have melting points below 0 °C and are stable at temperatures above 300 °C, but, due to the strong Coulombic interaction, are characterized by a negligibly low vapor pressure. The ease of product separation and catalyst recycling promises RTILs as replacements for conventional synthesis and separation processes and for electrochemical applications as in batteries and solar cells. Due to the largely diminished evaporation losses, they are often called "green solvents". The liquid-state dynamics of the RTILs is expected to be interesting because of the molecular nature of the ions. Moreover, specific design of such liquids for purposes such as targeted catalysis of a reaction, which is not possible using standard solvents, can probably be much facilitated by substantial knowledge of dynamics on a typical "molecular time scale" in the ultrafast time domain.

A steadily increasing number of studies on ultrafast dynamics in RTILs has been published over the past few years. The polarity of the commonly used liquids has been found to be comparable to that of highly polar conventional solvents such as acetonitrile or methanol.[3] Several time-resolved Kerr-effect studies[4−8] on imidazolium-based ionic liquids revealed a couple of Raman-active modes in the range of 30−150 cm^{-1}. The slowest relaxation time scales found in these experiments seem to correspond to those observed with conventional viscous liquids. The related dynamics have thus been attributed to diffusional motion. Neutron-scattering experiments[9] and Monte Carlo simulations[10] indicate the existence of three preferential positions for the anion around the imidazolium cationic ring. Wynne and co-workers[7] have attributed the observed Raman-active modes to a librational motion of the imidazolium ring against the anion in its different positions. Faster dynamics taking place on a few picosecond time scale seem, therefore, to origin from such kind of intermolecular oscillations.

Solvation dynamics of fluorescent probes in RTILs has been addressed by several groups. The observed time scales differ substantially from one publication to another, despite the similarity of the employed experimental techniques and the molecular systems under investigation.[11] Karmakar and Samanta[12−14] have reported on the dynamical Stokes shift of coumarin 153 (C153) and PRODAN in two substituted imidazolium salts using a time-correlated single-photon counting setup (TCSPC) with 50-ps time resolution. The observed time dependence of the emission maximum was reproduced with a double exponential function with time constants of $\tau_1 \approx 200$ ps and $\tau_2 \approx 1-1.2$ ns. The authors interpret these findings as an indication for a biphasic solvation dynamics involving a fast diffusional motion of the anion and a subsequent collective motion of the anion and the cation. Such biphasic solvation dynamics had already been proposed by Huppert and co-workers[15] for molten salts. Using stimulated emission and fluorescence up-conversion techniques in addition to TCSPC, Petrich and co-workers[16] have determined an additional fast component of about 7 ps, which they attribute to the "polarizability of the cation".

Maroncelli and co-workers[17−19] have also reported on the dynamic Stokes shift in different RTILs using TCSPC and various dye chromophores as solvation probes. The obtained results are compared with the large amount of solvation data on conventional polar liquids using C153 as a solute probe, collected by the same research group.[20] The rotational times found with the RTILs correlate with those of conventional polar aprotic solvents, and no significant change of the anisotropy is observed when measuring at different wavelengths over the emission band. In contrast to the other publications, the obtained time-dependent emission maximum is discussed in the framework of a stretched exponential function. The latter directly provides an average solvation time that is found to scale with viscosity as generally observed with conventional polar solvents. The authors interpret their results as a nonexponential solvation dynamics, involving a distribution of time scales, rather than

* To whom correspondence should be addressed. E-mail: eric.vauthey@chiphy.unige.ch.

† Present address: Departamento de Quimica Fisica, Facultad de Ciencias del Medio Ambiente, Universidad de Castilla-La Mancha, Avenida de Carlos III s/n, E-45007 Toledo, Spain.

10.1021/jp057482r CCC: $33.50
Published on Web 05/11/2006 PAGE EST: 6.9

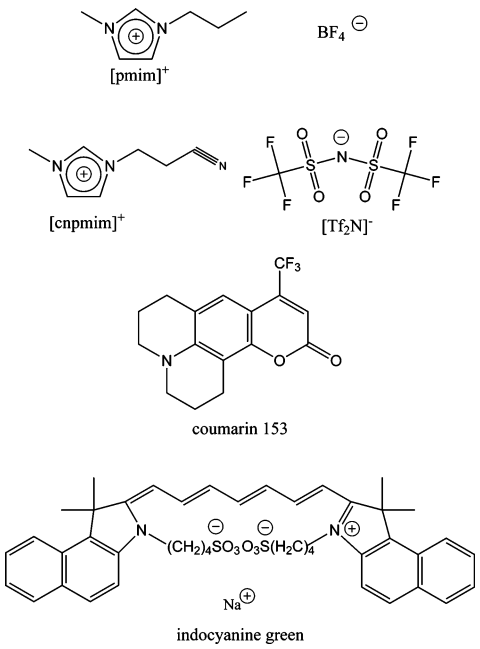

Figure 1. Ionic liquids and fluorescent probes.

biphasic dynamics. Comparing the spectral position of the emission maximum extrapolated to zero time delay with the position obtained for an apolar solvent of equal refractive index[21] yields a lack of 50% of the total Stokes shift for imidazolium liquids. This finding is interpreted by an unresolved ultrafast solvation component. Accordingly, 50% of the solvation dynamics should take place on a time scale faster than 5 ps. Interestingly, this hypothetical component seems to occur only in imidazolium liquids, but not in liquids based on phosphonium and ammonium cations.[19]

A major issue of the studies reported so far is the lack of sufficient time resolution for capturing dynamics occurring on the subpicosecond time scale. TCSPC is electronically limited to a response function of about 25 ps. Using deconvolution techniques, one can push the borderline in the best case by about half an order of magnitude. Dynamics beyond this limit remain unresolved. Only the stimulated emission experiments performed by Petrich and co-workers[16] permit a better time resolution. However, the presence of ground- and excited-state absorption tends to cover the emission dynamics in this experimental approach, and hence, the interpretation is difficult. In a very recent article, Maroncelli and co-workers[22] report on a Kerr-gate experiment with a 450-fs time resolution for measuring the early time solvation dynamics of DCS, which are unaccessible using TCSPC. However, due to the leak out on a longer time scale, only fluorescent probes with a relatively short excited-state lifetime can be employed, and thus, C153 cannot be used in such experiments.

In the present article, we focus on dynamic Stokes-shift measurements on C153 in two RTILs (see Figure 1) using the fluorescence up-conversion technique with a 230 fs response function. Complementary measurements with a recently completed up-conversion setup with even four times better time resolution support our finding that the ultrafast component of the solvation, though present, is not as important as presumed by Maroncelli and co-workers. Differences in conformation between polar and apolar environment could possibly induce an additional spectral shift, influencing thereby the estimation of the time-zero emission. Furthermore, the dynamical Stokes shift observed on a time scale of a few hundreds of femtoseconds using C153 as solute could possibly be hidden by probe-internal conformational changes.[23] First three-pulse photon-echo peak-shift experiments of the infrared dye indocyanine green in imidazolium liquids indicate a difference in the inertial part of the solvation dynamics as compared to the same dye molecule in ethanol. The decay of the initial signal is clearly slower in the imidazolium salt than in ethanol. Such very fast dynamics on a <100-fs time scale could partly account for the missing energy in the Stokes-shift experiments.

2. Experiment

The ionic liquids used in the experiments reported here, 1-(3-cyanopropyl)-3-methylimidazolium bis(trifluoromethylsulfonyl)-imide ([cnpmim$^+$][Tf_2N^-]) and 1-propyl-3-methylimidazolium tetrafluoroborate ([pmim$^+$][BF_4^-]), were synthesized by the group of Paul J. Dyson in Lausanne.[24,25] Coumarin 153 (C153, Radiant Dyes), indocyanine green, and dimethylanthracene (Fluka) were used as obtained. All liquids were stored under inert atmosphere. To speed up dissolution of the dyes, samples were heated to about 70 °C during 1−2 h. Before measurement, they were kept under vacuum to remove remainders of water. No further purification was performed. In the photon echo setup, solutions could be reused for several days without noticeable degradation. However, the relatively high viscosity of the RTILs limits circulation in spinning cells, and thus, samples in the up-conversion setup had to be changed after about 2 h of measurement.

The steady-state fluorescence spectra were measured in the reflective mode at concentrations that ensure an optical density of OD < 0.1 at the maximum of the C153 absorption band to minimize reabsorption effects. An intensity correction for the detection efficiency of the employed spectrometer ("Cary Eclipse", Varian) was obtained by comparing the emission spectra of a series of dyes with reference curves obtained using an intensity calibrated double monochromator spectrometer ("fluorolog", Jobin Yvon).

The early fluorescence dynamics of C153 was measured using a frequency up-conversion arrangement described in detail elsewhere.[26] Briefly, part of the output of a mode locked titanium-sapphire laser (Spectra Physics "Tsunami") is frequency doubled and is used to excite the sample at 400 nm. The fluorescence is gated by sum-frequency mixing with the fundamental of the oscillator output. The up-converted UV photons are directed into a monochromator and detected by a photomultiplier with subsequent single photon counting electronics. A step motor driven and 30 cm long optical delay line controls the time delay between excitation and gating. The sample solution is kept in a spinning cell of 0.4-mm thickness. The dye concentration was chosen such that the optical density of the sample was around 0.4 at the excitation wavelength. The laser intensity was kept low enough to minimize sample degradation. The response function of the up-conversion setup has a full width of half-maximum of 230 fs. Decay times longer than 1 ns have been measured using a TCSPC unit.[26] A pulsed laser diode with a wavelength of 395 nm and a repetition rate of 40 MHz is used as the excitation source for this arrangement. Its temporal resolution is presently limited to about 200 ps by the response time of the employed photomultiplier. All measurements were performed at environmental temperature stabilized to 19 °C.

For the photon-echo measurements, a cavity-dumped titanium−sapphire oscillator (KMLabs "Cascade") was used. A Bragg crystal inside the laser cavity dumps about 60% of the intracavity power at a tunable repetition rate between 20 kHz and 2 MHz. This permits one to obtain sufficient peak intensity without the

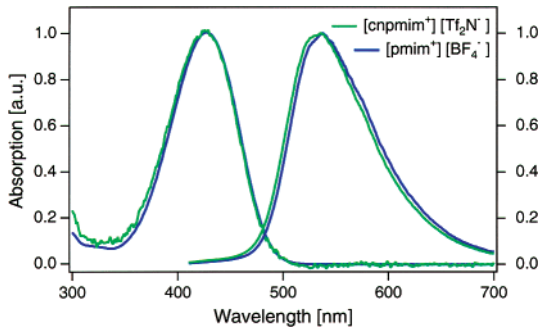

Figure 2. Steady-state absorption and emission spectra of C153 in [pmim$^+$][BF_4^-] and [cnpmim$^+$][Tf_2N^-].

need for an amplifying system and to avoid re-excitation of the illuminated sample spot by adjusting the repetition rate to the optical cycle of the chromophore probe. The oscillator yields typically 25 nJ per pulse at a central wavelength of 800 nm. The shortest obtainable pulses have a duration of about 15 fs. The dumped output-beam passes a quartz prism optical compressor, which compensates group velocity mismatch picked up on the way from the Bragg crystal to the sample cell. It is then split into three identical beams that are focused on the sample cell using a boxcars geometry. The widely employed triangular geometry could not be used here because it requires sample thicknesses smaller than the critical length—about 100 μm in our case—to avoid a significant phase mismatch. This turned out to be unfeasible due to the high viscosity of the ionic liquids. Quartz plates inserted into two of the three optical paths ensure a perfect dispersion match between the beams. The polarization of the beams is controlled by three identical $\lambda/2$ wave plates. After passing some irises to shield scattered light, the echo signal is integrally detected by a photodiode and digitized by a lockin-amplifier (Stanford Research SR530). A peristaltic pump circulates the sample solution through a 0.5 mm flow cell. The repetition rate and pulse energy were adjusted such that no thermal grating effects could be observed.

3. Fluorescence Measurements

Figure 2 shows the steady-state absorption and emission spectra of C153 in [pmim$^+$][BF_4^-] and [cnpmim$^+$][Tf_2N^-]. The absorption spectra are nearly identical, whereas the emission bands are shifted by about 10 nm. The shape is again practically identical and resembles closely the shape observed in conventional polar liquids such as short chain alcohols and acetonitrile. The maxima of the C153 emission band are situated at 523 and 534 nm in [cnpmim$^+$][Tf_2N^-] and [pmim$^+$][BF_4^-], respectively. In ethanol and hexanol, for instance, they are located at 527 and 518 nm. This indicates that the equilibrium solvation of the coumarin molecule in the RTILs used in this study differs not too much from what is known for conventional polar liquids. However, the shape of the absorption and emission bands looks clearly different in apolar liquids such as cyclohexane, where a double maximum structure is observed in the absorption band as well as in the emission band.

The dynamic Stokes-shift experiment was performed as described by Maroncelli and co-workers.[20] The temporal evolution of C153 fluorescence was measured at about 25 equidistant wavelengths over the emission band from 430 to 680 nm from small, negative time delays until 1 ns with a variable step size. Figure 3 shows the first 300 ps of three selected and normalized fluorescence transients on the high-energy side, the center, and the low-energy side of the emission band. A fast signal decay on the blue side and a corresponding rise on the red side of the

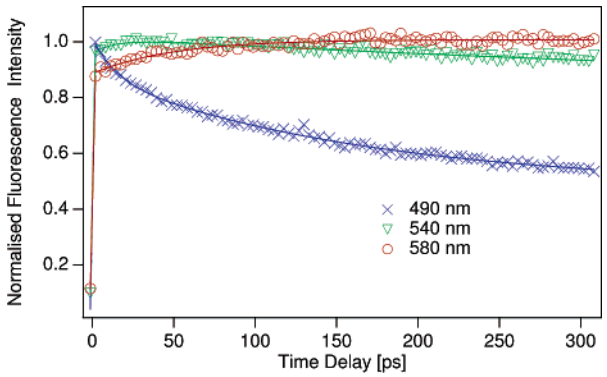

Figure 3. Normalized fluorescence time profiles on the blue edge, in the middle, and on the red edge of the emission band of C153 in [cnpmim$^+$][Tf_2N^-].

band is a characteristic feature of fluorescence emission during solvation processes and reflects the dynamic red-shift of the band. However, due to convolution with the instrumental response function, fast-rising components on the red side are often difficult to observe.

By means of a global fit analysis using a sum of exponential functions convoluted with a Gaussian function

$$F_\lambda(t) = Y_{0\lambda} + \frac{1}{\Delta_\lambda}\sum_{i=1}^{n} A_{i\lambda} \times \int_{-\infty}^{+\infty} \exp\left[-\left(\frac{t' - t_{0\lambda}}{\Delta_\lambda}\right)^2\right] \exp\left(-\frac{t' - t + t_{0\lambda}}{\tau_i}\right) dt' \quad (1)$$

the ensemble of the transient fluorescence signals can be represented analytically by four ([cnpmim$^+$][Tf_2N^-]) respectively five ([pmim$^+$][BF_4^-]) time constants, where $t_{0\lambda}$ and Δ_λ are time-zero and the width of the instrumental response function at the individual wavelengths, respectively. τ_i denote the set of global time constants and $A_{i\lambda}$ are the corresponding wavelength-dependent preexponential factors. The measured instrument response function of the employed setup can be reasonably well reproduced by a Gaussian function. In contrast to other functions, the convolution of an exponential decay with a Gaussian function can be performed analytically, thereby increasing the performance of the fitting procedure as the deconvolution has not to be included within the iteration loop of the fitting algorithm

$$F_\lambda(t) = Y_{0\lambda} + \sum_{i=1}^{n} \frac{A_{i\lambda}}{2} \exp\left(-\frac{t - t_{0\lambda}}{\tau_i}\right) \times \exp\left(\frac{\Delta_\lambda^2}{4\tau_i^2}\right)\left[1 + \mathrm{erf}\left(\frac{t - t_{0\lambda} - \Delta_\lambda^2/2\tau_i}{\Delta_\lambda}\right)\right] \quad (2)$$

The slowest time constant in the nanosecond range has been taken from the TCSPC experiment that did not show any dependence of this time constant on the emission wavelength. It was held fixed during the fit of the up-conversion data. Varying it by about 10−20% of its absolute value showed only little influence on the faster time constants of <1 ns, indicating a good separation of the time scales of solvation as opposed to population relaxation. Note that this fitting process is used to represent the set of measured fluorescence transients by analytical functions, which are easier to handle in the further evaluation

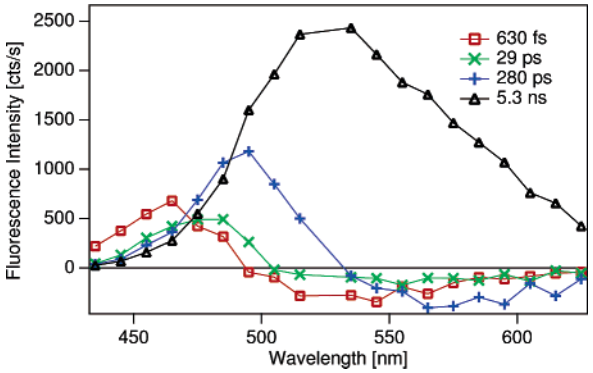

Figure 4. Preexponential factors obtained from global analysis of the ensemble of fluorescence time profiles of C153 in [cnpmim$^+$][Tf$_2$N$^-$].

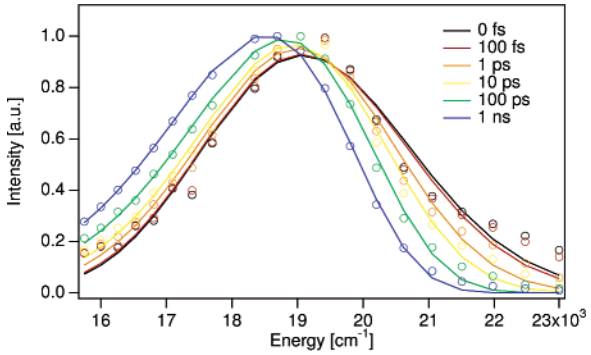

Figure 5. Reconstructed time-dependent emission spectra of C153 in [cnpmim$^+$][Tf$_2$N$^-$] at selected time delays after excitation. The solid lines are the results of a fit with log-normal functions.

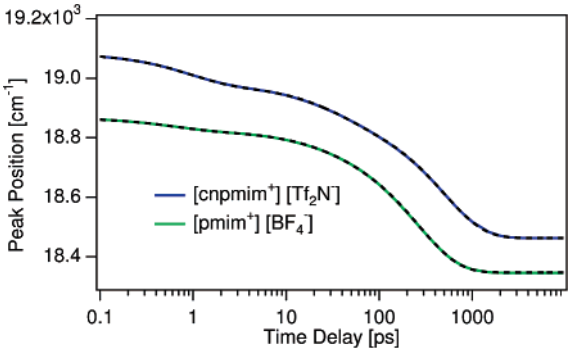

Figure 6. Time dependence of the emission band maximum of C153 in [pmim$^+$][BF$_4^-$] and [cnpmim$^+$][Tf$_2$N$^-$]. The dashed lines show the results of a fit with a triple exponential function.

procedure. No attempt is made to assign physical interpretation to the time scales and amplitudes by this first fit analysis.

Figure 4 depicts the ensemble of preexponential factors resulting from the global fit for [cnpmim$^+$][Tf$_2$N$^-$]. Positive values correspond to a decay, and negative ones correspond to a rise. The curves associated to the fast components exhibit a very similar shape, indicating a decay on the high-energy side and a rise on the low-energy side. These components are, thus, all to be attributed predominantly to a dynamic red-shift. Vibrational cooling, as opposed, leads to a band-narrowing, which would show up in this plot as a symmetric curve with positive values in the outer parts and negative values in the center. The absence of such a feature does not mean that narrowing due to cooling is absent here. However, none of the time constants obtained from the fit can be attributed exclusively to such process. On the other hand, the amplitude factors that belong to the longest time scale resemble closely the steady-state emission spectrum. Moreover, the time constant itself is of the same magnitude as the fluorescence lifetime of C153 observed in conventional polar solvents. This further supports that solvation dynamics is finished well before the relaxation of the chromophore to the ground state.

The results of the global fit can now be used to reconstruct the time-resolved fluorescence spectrum. Due to the spectral dependence of the up-conversion process and of the detection efficiency, the absolute signal intensities cannot be compared directly. A normalization to the integrated (steady-state) fluorescence intensities at the corresponding wavelengths is therefore necessary. In addition, the wavelength-dependent detection efficiency of the steady-state emission spectrometer has to be taken into account. After transformation to a scale linear in energy, which involves the multiplication by a factor $1/\nu^2$ to conserve the value of the total fluorescence yield,[27,28] the reconstructed spectra can be reproduced by so-called log-normal functions, which are commonly used to represent emission spectra in strongly polar solvents[20]

$$I(\nu, t) = \begin{cases} I_0 \exp\{-\ln(2)\,[\ln(1+\alpha)/\gamma]^2\} & \text{for} \quad \alpha > -1 \\ 0 & \text{for} \quad \alpha \le -1 \end{cases} \tag{3}$$

with

$$\alpha = 2\gamma(\nu - \nu_p)/\Delta \tag{4}$$

The four parameters I_0, ν_p, Δ, and γ describe the peak intensity, the peak position, the width, and the asymmetry of the band, respectively. Given that this class of functions reproduces well the reconstructed emission data, these four parameters may be used to fully characterize the dynamic Stokes shift.

Figure 5 shows a selection of reconstructed time-resolved emission spectra from very early emission towards the steady-state spectrum. On the blue edge, the early emission spectra cannot be reproduced as well as the later ones by such log-normal functions. However, the position of the peak maximum is well reproduced within the spectral resolution of 10 nm. Whether the first and higher moments calculated from the whole set of corresponding parameters represent the experimental data sufficiently well is more difficult to judge. The far blue edge of the emission spectrum is difficult to measure with satisfying signal-to-noise ratio due to the weak absolute signals for both time-resolved and steady-state measurements. Moreover, during the interaction with the pump pulse, a relatively strong signal induced by Raman scattering in the solvent is superimposed to the fluorescence and further increases the uncertainty. We will therefore rely on the peak position ν_p, as in the majority of studies published in the field.

Figure 6 shows the peak frequency of the emission band as a function of time for C153 in [cnpmim$^+$][Tf$_2$N$^-$] and [pmim$^+$][BF$_4^-$] as resulting from the log-normal fits. Normalized to the total Stokes shift, such a representation is often referred to as Stokes-shift correlation function[29]

$$C(t) = \frac{\nu(t) - \nu(\infty)}{\nu(0) - \nu(\infty)} \tag{5}$$

Apart from an overall shift in energy, the two obtained curves resemble each other. The difference varies between 160 cm^{-1} during the first picosecond and above 200 ps, and around 120 cm^{-1} on the intermediate time scale, which corresponds to about 10% relative variation compared to the total observed Stokes shift. It seems, therefore, that neither the nature of the two different anions nor the presence or absence of the cyano group

TABLE 1: (a) Results of a Triple Exponential Fit Analysis of the Time-Dependent Peak Position, (b) Results of a Stretched Exponential Fit Analysis of the Same Set of Data Starting at 2 ps, and (c) Average Solvation Times Calculated from the Two Fits and Estimated Viscosities of the Employed RTILs

(a)	$[pmim^+][BF_4^-]$	$[cnpmim^+][Tf_2N^-]$
A_{01} [cm^{-1}]	430	410
τ_1 [ps]	270	490
A_{02} [cm^{-1}]	48	110
τ_2 [ps]	26	32
A_{03} [cm^{-1}]	43	100
τ_3 [ps]	0.62	0.90

(b)	$[pmim^+][BF_4^-]$	$[cnpmim^+][Tf_2N^-]$
A_0 [cm^{-1}]	530	480
τ [ps]	340	230
β	0.68	0.87

(c)	$[pmim^+][BF_4^-]$	$[cnpmim^+][Tf_2N^-]$
$\langle\tau_{solv}\rangle_{3e}$ [ps]	225	330
$\langle\tau_{solv}\rangle_{se}$ [ps]	245	445
η [cP]	30−40	70−90

on the cation plays a dominant role in the solvation dynamics in these two liquids. However, minor differences in the shape are present.

The dashed lines in Figure 6 are the results of a fit analysis using a triple exponential function. Less than three exponential terms do not properly reproduce the experimental data. The corresponding parameter values are given in Table 1. The average solvation time resulting from these values has been calculated as

$$\langle\tau_{solv}\rangle_{3e} = \sum_{n=1}^{3} A_{0n}\tau_n$$

and

$$\sum_{n=1}^{3} A_{0n} \equiv 1 \qquad (6)$$

For comparison, we have also performed a fit analysis using a stretched exponential function

$$\nu(t) = \nu(\infty) + \Delta\nu \exp\{-(t/\tau_0)^{\beta}\} \qquad (7)$$

When omitting the first two picoseconds, the fit is close to perfect for $[pmim^+][BF_4^-]$ and of a bit lesser quality for $[cnpmim^+][Tf_2N^-]$. On the other hand, when including the early part, the results of the fits are rather poor. As being obvious from the plot, the kink around 2 ps cannot be captured by a single stretched exponential function. However, also when using a sum of two stretched exponential terms, the fit algorithm does not properly converge. The observed early-time feature might be due to a change in character of the relaxational motion or due to the presence of chromophore-internal dynamics, as will be discussed later. Stretched exponential functions can also be used to specify an average relaxation time defined as[20]

$$\langle\tau_{solv}\rangle_{se} = \frac{1}{\Delta\nu}\int_0^{\infty}[\nu(t) - \nu(\infty)]dt = \frac{\tau_0}{\beta}\Gamma(1/\beta) \qquad (8)$$

where Γ is the gamma function. This yields an average solvation time of 445 ps for C153 in $[cnpmim^+][Tf_2N^-]$ and of 245 ps in $[pmim^+][BF_4^-]$ for the solvation dynamics from 2 ps until the complete relaxation. Comparing the values of the average solvation time obtained by the two methods, we find a good agreement with $[pmim^+][BF_4^-]$. The difference with $[cnpmim^+][Tf_2N^-]$ is most probably due to the early component that could not be included in the stretched exponential fit and would diminish the obtained result by some amount.

Compared to the studies on the dynamic Stokes shift cited before, the values obtained here are relatively small. However, when changing from one solute probe to another without changing the laboratory conditions, changes of the same order of magnitude have been observed.[11] A further role might play the length of the carbon chain. All other studies rely on methyl-, ethyl-, and butyl-substituted imidazolium salts. The average relaxation time of butyl-imidazolium is found to scale with the viscosity.[18] A more precise measurement of the viscosity of the RTILs investigated in this study will be presented in a forthcoming publication. Here, we give an estimation based on a comparison of the fluorescence anisotropy of dimethylantracene in the two RTILs with values obtained for ethylene glycol and decanol where the viscosity is known. The choice of the chromophore was due to the relatively high viscosity of the RTILs. To obtain meaningful results, it is essential that the fluorescence lifetime of the chromophore well extends the time scale of rotational diffusion. The estimation leads to a viscosity of 30−40 cP for $[pmim^+][BF_4^-]$ and of 70−90 cP for $[cnpmim^+][Tf_2N^-]$. A comparison with values published for other imidazolium salts[17] shows good agreement with our findings.

A major issue when calculating the average relaxation time as well as the Stokes-shift correlation function is the estimation of the total spectral shift of the emission band. $\nu(t = \infty)$ can easily be obtained from the steady-state emission spectrum, as long as the solvation relaxation is sufficiently faster than the fluorescence lifetime. On the other hand, $\nu(t = 0)$ represents the center of a spectrum obtained from a vibrationally entirely relaxed but otherwise completely unsolvated chromophore. Such a hypothetical situation cannot be realized experimentally as the internal relaxation starting from the Franck−Condon configuration and the onset of the solvation-relaxation, especially the inertial component of the latter, are superimposed at early times upon impulsive excitation. Fee and Maroncelli propose an estimation of $\nu(t = 0)$ by quantitatively comparing the pair of excitation−emission spectra in the polar solvent under investigation with the bands of the same chromophore in an apolar reference solvent.[21] On the basis of this method, Maroncelli and co-workers suppose the existence of a contribution to the solvation being faster than 5 ps in imidazolium liquids,[17−19] which should account for 50% of the total dynamical Stokes shift. However, such an estimation relies on the assumption that the ground state structure of the chromophore remains invariant when changing from one solvent to another, where one has especially to bear in mind that C153 has already a quite high permanent dipole in its ground state.[30] As the character of solute−solvent interaction changes when changing from a polar to an apolar environment, changes of the geometrical structure of the chromophore corresponding to a shift in the order of some hundreds of wavenumbers cannot be completely ruled out. Furthermore, gas-phase simulations and experiments[23] indicate a conformational change of the C153 molecule within the first several hundreds of femtoseconds after photoexcitation. Whether such a change also occurs in the condensed phase and to which extent it could influence the result of Stokes-shift measurements has not been subject to explicit investigation up to now.

In the present study, the part of the solvation taking place on the time scale up to 10 ps accounts for about 10−20% of the total shift. Not being negligible, this is less than the proposed

50%. The fastest time constant necessary to properly reproduce the early part of the fluorescence transients in the blue wing of the emission spectrum equals ca. 500 fs for [pmim$^+$][BF_4^-]. The weight of this component, given by the corresponding preexponential factor, is far from being large enough to establish a more substantial ultrafast component. To further support this finding, we have measured again the blue wing of the emission band using a recently completed up-conversion setup, which employs all-reflective optics and therefore has a sharper response function of 85-fs width. The resulting fastest time constant gets smaller by about 10%. A simple estimation shows that a missing shift of 1000−1500 cm^{-1} would have to take place within less than 15−25 fs to remain invisible with the improved time resolution. However, smaller changes of the emission peak frequency could remain invisible on a slightly longer time scale. Furthermore, the deviance in the high-energy wing between the reconstructed spectra and the log-normal functions resulting from the fit may influence the extrapolated time-zero emission-peak frequency. It has to be stressed that a spectral spacing of the transients of 10 nm around 500 nm corresponds to a spacing of 400 cm^{-1} around 20 000 cm^{-1}. A resolution beyond this value asks for an extremely good fit of the model function to the experimental data, especially when taking into account the relative incertitude of the absolute fluorescence yield in the blue wing of the emission spectrum, which is due to the early-time dynamics. At the present signal-to-noise ratio, the absolute Stokes-shift amplitudes have thus to be taken with care, whereas the obtained time scales should remain significant. A superposition of the four discussed effects, (a) conformational changes of the solute ground-state structure between polar and apolar environments, (b) dynamical conformation changes upon excitation to the Franck−Condon state, (c) ultrafast (inertial) solvent relaxation, and (d) some inaccuracy of the log-normal representation of the early fluorescence may possibly explain the energy mismatch observed with imidazolium salts. For further information on the evaluation procedure and its limitations, see the Supporting Information.

In recapitulation, the question about the origin of the mismatch between the estimation of $\nu(t = 0)$, using a comparison with an apolar solvent, and the time-resolved data in all experiments so far reported on imidazolium-based RTILs must remain unanswered for the moment. Further studies are needed to clarify the influence of the solute probe, especially at very early times. Our results furthermore demonstrate that time resolution in the sub 100-fs time scale is necessary to address these questions.

4. 3PEPS Measurements

The relatively high incertitude of Stokes-shift amplitudes at early times under our present experimental conditions and the difficulty to disentangle the diversity of dynamical processes taking place in parallel on the ultrafast time scale led us to consider a different attempt to solvation dynamics in RTILs. Figure 7 shows first results of a three-pulse photon-echo peak-shift (3PEPS) measurement on indocyanine green in [cnpmim$^+$][Tf_2N^-] and in ethanol during the first half picosecond. At present, the setup is limited to an excitation wavelength of 800 nm. Therefore, a chromophore different from that used in Stokes-shift measurements had to be employed. The 3PEPS technique is known to directly yield, in many cases, the system−bath correlation function[31,32]

$$M(t) = \frac{\langle \delta\omega(0)\delta\omega(t)\rangle}{\langle \delta\omega^2\rangle} \tag{9}$$

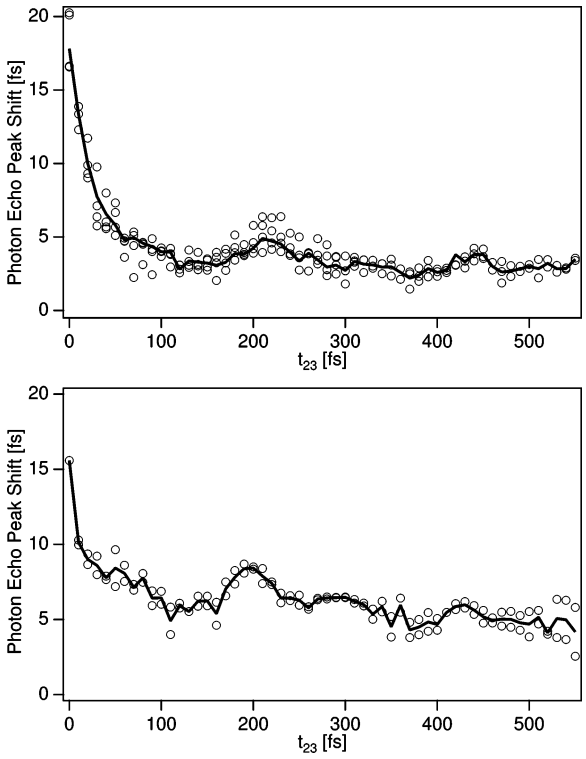

Figure 7. First three pulse photon-echo peak-shift measurements of indocyanine green in [cnpmim$^+$][Tf_2N^-] (top) and in ethanol (bottom). The solid lines are the average over the results of several subsequent scans.

This function describes the solute−solvent interaction on the basis of transition frequency fluctuations, whereas the Stokes-shift correlation function $C(t)$ addresses the same physical process by means of energy dissipation. At high temperatures, theoretical considerations show that $M(t)$ and $C(t)$ should be essentially identical,[32] except for the region around time-zero where the laser pulses still overlap. In the latter case, 3PEPS traces contain contributions from interactions with time-inverted order of the incoming laser beams. The interference between the corresponding additional Liouville pathways prevents a straightforward interpretation of the experimental results close to time-zero.[33]

The overall shape of the obtained curves for the RTIL and ethanol look similar. A fast decay during the first 100 fs is followed by some oscillatory structure that is superimposed to a decay on a 5-ps time scale and a longer tail (not shown here). The peaklike feature at 200 fs and a potential recurrence at 400 fs indicate a coherent rephasing and could be either due to an intramolecular wave packet or due to a solvent mode. The fact that this feature occurs in both liquids investigated here, as well as with other infrared dyes of similar structure,[34] points toward an intramolecular mode. Whether the offsetlike tail of the signal represents a slower component of the solvent reorganization or is due to a problem of alignment cannot be distinguished at the present signal-to-noise level. The fast initial decay, on the other hand, does not look the same for the RTIL and ethanol. In the RTIL, the signal starts at a higher level and decays slower than in ethanol. This could indicate a difference in the inertial part of the solvent response. Such a process during the first 20−40 fs could account for a part of the solvation energy missed in the Stokes-shift measurements.

As stated before, a direct interpretation of this early part of the 3PEPS trace is difficult without accompanying simulations. Solute−solvent correlation functions, which have been calcu-

lated by MD methods using a small solute-probe,[35] show qualitative agreement with the results obtained here. Improved data quality, extension of the Stokes-shift measurements to the IR spectral region, and model calculations exactly on the system experimentally investigated will be necessary for a better understanding. Extending the 3PEPS measurements to some 100 ps with sufficient signal-to-noise ratio and measuring the dynamic Stokes shift of the same dye in the same environment at the same excitation wavelength should provide both a test of theoretical predictions upon the identity of the two correlation functions $C(t)$ and $M(t)$ and a cross check of the amplitude accuracy of dynamic Stokes-shift measurements on the early emission.

5. Summary

The dynamic Stokes shift of coumarin 153 in the two RTILs [cnpmim$^+$][Tf_2N^-] and [pmim$^+$][BF_4^-] has been measured using fluorescence up-conversion techniques with a response function of 230 fs. The better time-resolution with respect to the majority of other studies on imidazolium-based RTILs allows us to address directly the early part of the emission. Being in accordance with the findings of other works on the picosecond time-domain, we can report also the dynamical Stokes shift time-resolved down to 100 fs. This results in an estimated contribution of the ultrafast component (100 fs−10 ps) on the order of 10−20% of the total solvation energy, as opposed to 50% which has been supposed earlier for C153 as the solvation probe. The question of why the estimation of the peak emission at time-zero by comparing absorption−emission spectra in apolar solvents differs from the time-zero peak position extrapolated from time-resolved measurements needs further investigation. Possible reasons could be combinations of (a) differences in the (ground-state) solute−solvent interaction, introducing an additional spectral shift which is not considered when comparing absorption−emission spectra in polar and apolar solvents, (b) chromophore-internal conformational changes during the first 100 fs, (c) unresolved inertial relaxation components, and (d) problems in capturing sufficiently well the blue wing of the fluorescence emission at very early times.

First three-pulse photon-echo peak-shift experiments on indocyanine green in RTILs are in qualitative agreement with MD simulations in similar molecular systems. A comparison using ethanol as solvent indicates a difference in the inertial part of the solvation relaxation between RTIL and ethanol. A comparison of the complementary 3PEPS and dynamic Stokes-shift measurements using the same chromophore−solvent conditions in future should yield a more comprehensive picture of the entire solvation dynamics.

Acknowledgment. We thank Paul J. Dyson for providing the ionic liquids, Andreas Hauser for the possibility of using his intensity calibrated fluorescence spectrometer, Mark Maroncelli for the useful hints on the data evaluation, and the Swiss National Science Foundation for the financial support (Project No. 200020-107466).

Supporting Information Available: Simulated fluorescence emission for verifying the evaluation routines and testing the limits of the employed reconstruction method. Discussion of the limits of the reconstruction method under present experimental conditions. This material is available free of charge via the Internet at http://pubs.acs.org.

References and Notes

(1) Welton, T. *Chem. Rev.* **1999**, *99*, 2071.
(2) Wasserscheid, P., Welton, T., Eds. *Ionic Liquids in Synthesis*; Wiley−VCH: Weinheim, 2003.
(3) Aki, S. N. V. K.; Brennecke, J. F.; Samanta, A. *Chem. Commun.* **2001**, *5*, 413.
(4) Shirota, H.; Funston, A. M.; Wishart, J. F.; Castner, E. W., Jr. *J. Chem. Phys.* **2005**, *122*, 184512.
(5) Shirota, H.; Castner, E. W., Jr. *J. Phys. Chem. A* **2005**, *109*, 9388.
(6) Shirota, H.; Castner, E. W., Jr. *J. Phys. Chem. B* **2005**, *109*, 21576.
(7) Giraud, G.; Gordon, C. M.; Dunkin, I. R.; Wynne, K. *J. Chem. Phys.* **2003**, *119*, 464.
(8) Hyun, B.-R.; Dzyuba, S. V.; Bartsch, R. A.; Quitevis, E. L. *J. Phys. Chem. A* **2002**, *106*, 7579.
(9) Hardacre, C.; Holbrey, J. D.; McMath, S. E. J.; Bowron, D. T.; Soper, A. K. *J. Chem. Phys.* **2003**, *118*, 273.
(10) Hanhe, C. G.; Price, S. L.; Lynden-Bell, R. M. *Mol. Phys.* **2001**, *99*, 801.
(11) Ito, N.; Arzhantsev, S.; Maroncelli, M. *Chem. Phys. Lett.* **2004**, *396*, 83.
(12) Karmakar, R.; Samanta, A. *J. Phys. Chem. A* **2002**, *106*, 4447.
(13) Karmakar, R.; Samanta, A. *J. Phys. Chem. A* **2002**, *106*, 6670.
(14) Karmakar, R.; Samanta, A. *J. Phys. Chem. A* **2003**, *107*, 7340.
(15) Bart, E.; Meltsin, A.; Huppert, D. *J. Phys. Chem.* **1994**, *98*, 10819.
(16) Chowdhury, P. K.; Halder, M.; Sanders, L.; Calhoun, T.; Anderson, J. L.; Armstrong, D. W.; Song, X.; Petrich, J. W. *J. Phys. Chem. B* **2004**, *108*, 10245.
(17) Arzhantsev, S.; Ito, N.; Heitz, M.; Maroncelli, M. *Chem. Phys. Lett.* **2003**, *381*, 278.
(18) Ingram, J. A.; Moog, R. S.; Ito, N.; Biswas, R.; Maroncelli, M. *J. Phys. Chem. B* **2003**, *107*, 5926.
(19) Ito, N.; Arzhantsev, S.; Heitz, M.; Maroncelli, M. *J. Phys. Chem. B* **2004**, *108*, 5771.
(20) Horng, M. L.; Gardecki, J. A.; Papazyan, A.; Maroncelli, M. *J. Chem. Phys.* **1995**, *99*, 17311.
(21) Fee, R. S.; Maroncelli, M. *Chem. Phys.* **1994**, *183*, 235.
(22) Arzhantsev, S.; Jin, H.; Ito, N.; Maroncelli, M. *Chem. Phys. Lett.* **2006**, *417*, 524.
(23) Mühlpfordt, A.; Schanz, R.; Ernsting, N. P.; Farztdinov, V.; Grimme, S. *Phys. Chem. Chem. Phys.* **1999**, *1*, 3209.
(24) Dyson, P. J. *J. Am. Chem. Soc.* **2004**, *126*, 15876.
(25) Zhao, D.; Fei, Z.; André, C.; Laurency, G.; Dyson, P. J. *Chem. Commun.* **2004**, *21*, 2500.
(26) Morandeira, A.; Engeli, L.; Vauthey, E. *J. Phys. Chem. A* **2002**, *106*, 4833.
(27) Birks, J. B. *Photophysics of Aromatic Molecules*; Wiley-Interscience: London, 1970.
(28) Angulo, G.; Grampp, G.; Rosspeintner, A. *Spectrochim. Acta, Part A* **2006**, *65*, 727.
(29) Nagarajan, V.; Brearley, A. M.; Kang, T.-J.; Barbara, P. F. *J. Chem. Phys.* **1987**, *86*, 3183.
(30) Cave, R. J.; Castner, E. W., Jr. *J. Phys. Chem. A* **2002**, *106*, 12117.
(31) de Boeij, W. P.; Pshenichnikov, M.; Wiersma, D. A. *Chem. Phys. Lett.* **1996**, *253*, 53.
(32) Cho, M.; Yu, J. Y.; Joo, T. H.; Nagasawa, Y.; Passino, S. A.; Fleming, G. R. *J. Phys. Chem.* **1996**, *100*, 11944.
(33) Mukamel, S. *Principles of Nonlinear Optical Spectroscopy*; Oxford University Press: Oxford, 1995.
(34) Passino, S. A.; Nagasawa, Y.; Joo, T.; Fleming, G. R. *J. Phys. Chem. A* **1997**, *101*, 725.
(35) Shim, Y.; Choi, M. Y.; Kim, H. J. *J. Chem. Phys.* **2005**, *122*, 044511.